Study of Phase Changes in Plasma Sprayed Deposits

P. Chraska, J. Dubsky, B. Kolman, J. Ilavsky, and J. Forman

The formation of a plasma-sprayed coating that exhibits predictable properties requires the control of many process variables. The phase changes that take place during plasma spraying are significant material variables that should be controlled. Several different materials were deposited in air with a water-stabilized plasma torch (model PAL 160). Usually, air was used as a carrier gas for the powder; however, argon was also used for some coatings. The injected powders (NiAl, Ni, $ZrSiO_4$-based, Al_2O_3-based, etc.) as well as the coatings were studied for, among other properties, their structure, particle size, microhardness, and chemical and phase composition. Phase changes induced by the different cooling rates of molten particles after their impact on a substrate are illustrated for $ZrSiO_4$. It has also been found that the oxidizing power of the water-stabilized torch is less than previously believed. For example, coatings produced with nickel powder injected with argon as the carrier gas exhibited almost no oxides. Significant element redistribution during plasma spraying was demonstrated with a two-phase NiAl feedstock powder. The coating exhibited almost all the phases that are present in the binary NiAl alloy as well as envelopes of oxides and traces of amorphous phase.

1. Introduction

PLASMA-SPRAYED coatings are widely used in many fields of technology, and therefore, considerable effort is aimed toward the description, understanding, and control of particular processes and mechanisms governing their formation and properties. Many material properties are dependent not only on chemical composition, but also on the microstructure and phase composition. There are many process variables that determine the spraying output; however, usually any particular property is often achieved through a chemical modification of the injected powder. Concentrations of stabilizing elements in a certain powder may be optimized, but this is frequently considered from the equilibrium viewpoint, whereas plasma spraying is a nonequilibrium process.

A great variety of phase changes take place during plasma deposition.[1,2] From the practitioners point of view, these phase changes can sometimes be beneficial; at other times, they are detrimental. Hence, it is important to study all of the possible phase changes occurring during plasma deposition, particularly because some of these have been neglected in the past. This article describes results obtained from detailed phenomenological studies of several metallic and ceramic materials. The phase content determination is further complicated because there is texturing of the deposits.[3]

Key Words: alumina, Ni, NiAl, NiTi, phase changes, water stabilized plasma, zircon

P. Chraska, J. Dubsky, B. Kolman, and **J. Forman,** Institute of Plasma Physics Czechoslovak Academy of Sciences, Prague, Czechoslovakia; and **J. Ilavsky,** Thermal Spray Laboratory, SUNY at Stony Brook, New York.

2. Basic Considerations

Several remarks concerning phase changes can be made from examination of the plasma spray experimental setup. The process zone is divided into several stages, as proposed, for instance, by Fauchais *et al.*[4] The first phase change takes place after the solid powder is injected into the plasma torch, *i.e.*, melting. It has been pointed out, for instance,[5] that the degree of melting is very important for the final density of deposits. More experimental work is required on the injected particle/plasma jet interactions, particularly with regard to heat transfer problems. Another problem touches the selective evaporation of certain elements or entire particles in the plasma stream. Finally, a question must be raised as to how the geometrical setup of the powder injection mode can affect the phase composition of the final deposit.

The phase change from solid to liquid at the start of the process is self-evident; however, so are the phase changes of solidification after impact of particles on the substrate. The phase structure depends not only on the chemical composition of the powder, but also on process variables such as plasma enthalpy, velocity of the particles, temperature of the substrate, and above all the heat transfer conditions between the particle and substrate, or particle and the previously deposited layer(s). For instance, the heat transfer conditions will differ considerably between the first layer of splats that come in contact with a highly conducting substrate and the following layers of splats that are mixed with pores, unmelted particles, and many other microstructural features. Thus, it is reasonable to expect differences in the phase content of regions adjacent to the interface between the deposit and substrate and regions farther away from this interface. Finally, it remains to be established whether any phase changes can occur during the short time of flight of molten or partially molten particles before their impact.

Because many material properties are sensitive to the type of the structure and the phase content, it is very important to study

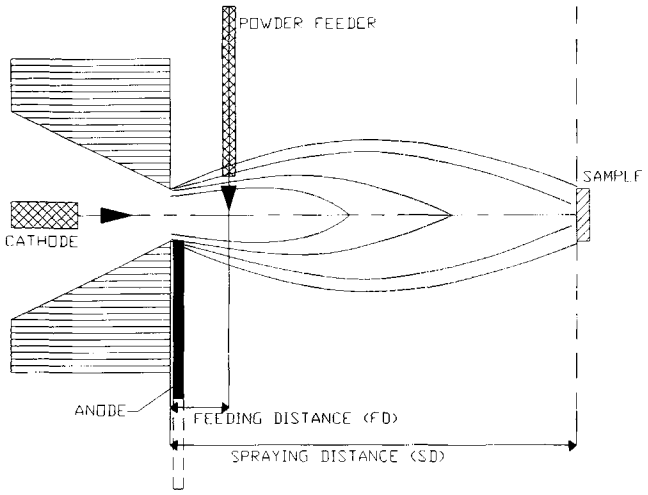

Figure 1 Schematic of spraying by a PAL 160 plasma torch.

relations between the feedstock powder state and that of the sprayed materials. Control of the structure and phase composition of the sprayed products would lead to a possible prediction of its final properties.

3. Experimental Procedures

The majority of materials studied in this work were deposited in air by the Czechoslovak water-stabilized plasma torch model PAL 160 (operating voltage of 310 to 340 V, current 460 to 490 A, and enthalpy of $\sim 0.2 \times 10^5$ J · kg^{-1}). The prime operational parameters adjusted were the torch-to-substrate spray distance (*i.e.*, SD) and the distance between the torch and powder injector (*i.e.*, the feeding distance or FD), as shown in Fig. 1. Usually, air was used as a carrier gas for the powder feeding, but a limited comparison with argon carrier gas was also made. A carbon steel or graphite was used as the substrate. The particle size distributions of the powders were routinely measured.

This gun, with 160-kW power, was capable of high powder throughput (about 50 kg · h^{-1} for alumina), and this corresponds to a coating thickness of about 0.3 mm for a single pass. Thicker deposits up to 6 mm may be formed by multiple passes. Free-flight particles were obtained by spraying into water placed at approximately the same distance as the solid substrate.

Deposits were studied either on or removed from the substrate, and both cross sections and the free surface were examined. Three methods were used for preparation of samples from the feedstock powders and the free-flight particles—(1) gluing on a layer of Leit-C conductive material, (2) dispersing in resin, cutting and polishing, and (3) fixing with collodion for X-ray study. Light microscopy (LM), scanning electron microscopy (SEM), and transmission electron microscopy (TEM) were used for structural and morphological characterization. Local chemical analysis using X-ray microanalysis (XMA) with energy as well as use of a wavelength dispersive analyzer of X-ray and energy dispersive (ED) X-ray fluorescence analyzer (XRF) were used for chemical concentration and elemental distribution studies. Phase composition was determined by X-ray diffraction

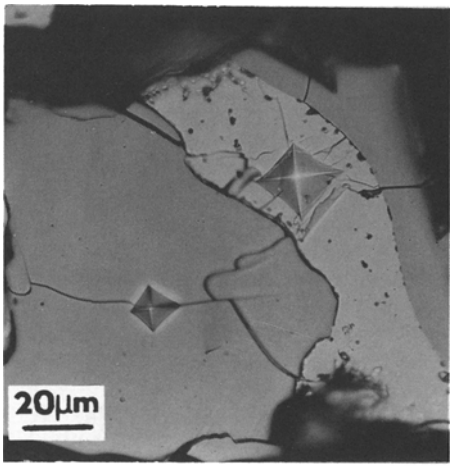

(a)

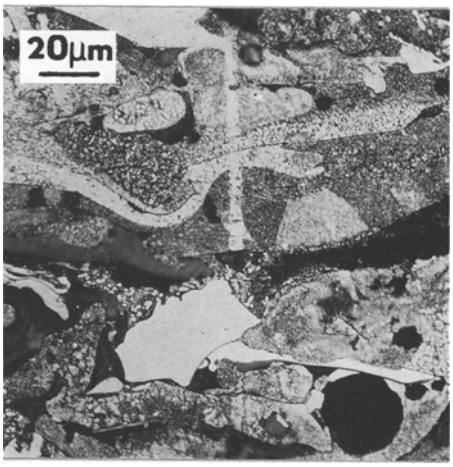

(b)

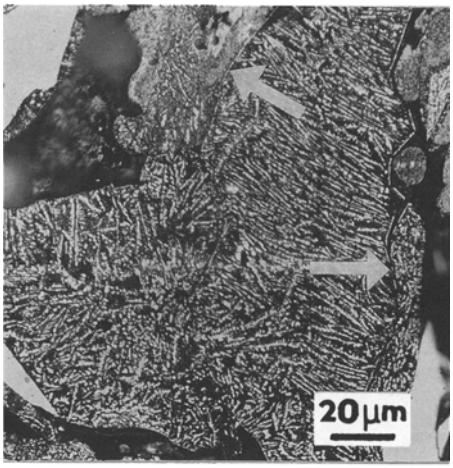

(c)

Figure 2 **(a)** NiAl original powder, showing two phases with different hardness. **(b)** NiAl plasma-sprayed deposit. **(c)** Oxides envelopes in NiAl deposit (arrows).

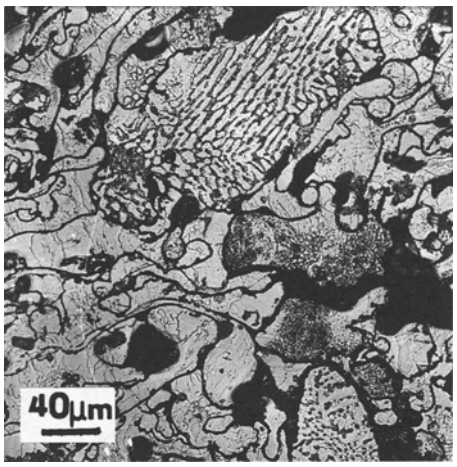

Figure 3 Eutectic in aluminum-silicon deposit.

techniques (XRD) or by selected area electron diffraction (SAD) during TEM. Finally, Vickers microhardness (HV) of different structures and phases was determined.

4. Phenomenological Description of Phase Changes

The following section presents examples of various phase changes observed in the plasma spraying process. Similar processes may also take place in other materials and systems. This work compares the original powders, free-flight particles, and deposits of the same nature. Several phenomenological conclusions are drawn which are of practical use for plasma spraying, as well as worthy of further research.

4.1 *Formation of Many Phases from a Few: NiAl*

The feedstock powder (Fig. 2a) was pulverized from an alloy of nominal composition 40 wt% Ni and 60 wt% Al. Two different particle size fractions were present: less than 45 µm and 100 to 200 µm in diameter. A deposit of NiAl about 1 mm thick was sprayed onto graphite (Fig. 2b). A comparison of the feedstock material and the deposit was performed. Detailed experimental conditions are presented in Ref 2.

Analysis by XRD combined with LM and VHM measurements showed that there was a mixture of two phases in the initial powder. These phases of $NiAl_3$ and Ni_2Al_3 were distributed homogeneously with no relation to the particle size. However, an analysis of the deposit showed that, with the exception of Ni_3Al, all other phases from the Ni-Al phase diagram were present, *i.e.*, Ni and αNi, NiAl, Ni_2Al_3, $NiAl_3$, and Al.

When air was used as a carrier gas, up to 15 vol% oxides (mainly in the form of envelopes around grains, Fig. 2c) were found in addition to the other phases in the structure. The deposits prepared with argon carrier gas did not exhibit significant amounts of oxide. Finally, traces of an amorphous phase were detected. This result suggests that a significant element redistribution must have taken place during the plasma spraying process. However, due to the complexity of the process, it is not possible to define the precise mechanisms or the time evolution of the phases.

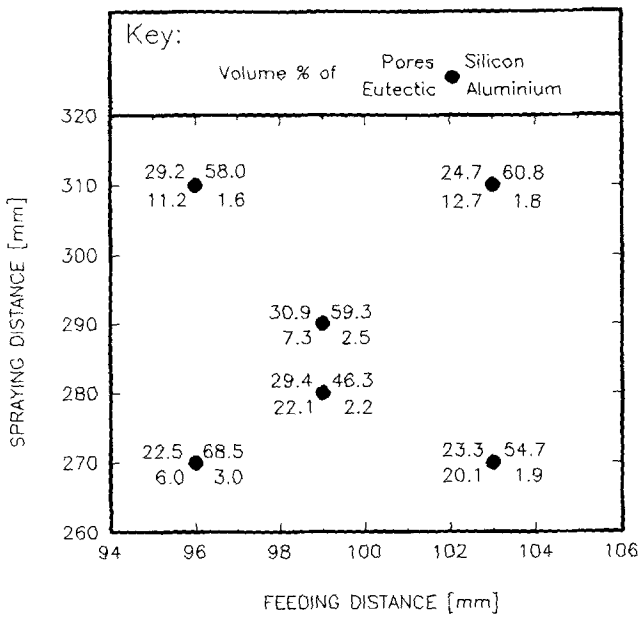

Figure 4 Volume fraction of eutectic, pores, aluminum, and silicon contents, and the dependency on the experimental spraying setup.

4.2 *Processes Occurring during Flight*

4.2.1 *Chemical Recombination: Al + Si; Al_2O_3 + TiO_2*

Silicon powder with a grain size of 70 to 120 µm and Al powder (90 to 160 µm) were mechanically mixed (volume ratio 1 to 9) and sprayed on a graphite substrate (0.6 to 0.7 mm thick deposit) or into water.[6] In both cases, a significant amount of AlSi eutectic was formed (Fig. 3). The detection of this eutectic in the free flight particles suggests that the molten droplets of aluminum and silicon were able to combine and react in about ~0.5 ms, the flight time of particles. This conclusion is supported by the observation that the lengthening of the flight distance brought an increase in the eutectic volume (Fig. 4).

Alumina-based powders with TiO_2 can be prepared using several methods, for example, by agglomeration with a binder. In the present case, the injected powder contained the trigonal αAl_2O_3 phase, the anatase modification of TiO_2, and a small amount of βAl_2O_3. It can be noted that the β-alumina is stabilized by Na_2O and therefore should be expressed as $xNa_2O \cdot yAl_2O_3$. After spraying, however, either in the deposit or in the free-flight particles, very little TiO_2 was found by XRD as a distinct phase in the rutile modification. Most of the TiO_2 was incorporated within the Al_2O_3 solid solution.[7,8]

4.2.2 *Selective Burning Out or Evaporation: Al_2O_3-Based Powders*

Some phase differences between the injected powder and the resulting deposit may be induced by altering the original chemical composition. Referring to the same example as in Section

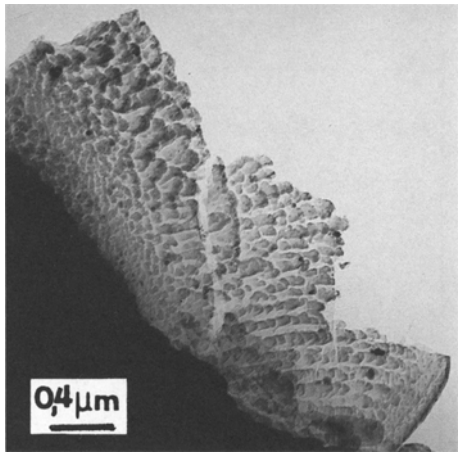

Figure 5 TEM of a splat from the first deposited layer of $ZrSiO_4$.

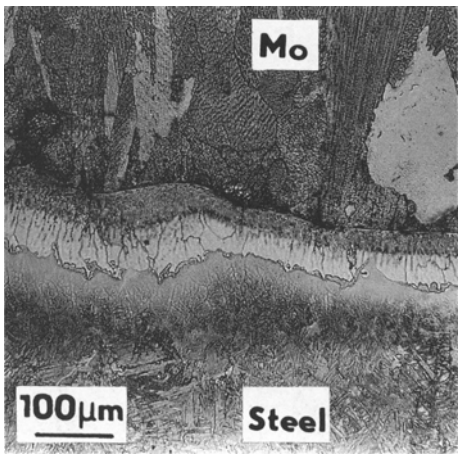

Figure 6 Phase distributions at the interface of a molybdenum droplet/steel.

4.2.1, no traces of βAl_2O_3 were found by XRD after spraying. Chemical analysis established that the content of Na_2O decreased by at least one order of magnitude, which is beneficial. The second result from XMA and XRF shows that the amount of TiO_2 was reduced by as much as 70% of its original value.[7]

4.2.3 *Oxidation: Al, Ni, NiAl, NiTi, NiBSi, and NiCrAl*

The water-stabilized plasma jet has been presumed to be a strong oxidizing medium. However, results on several types of metallic powder show that the oxidizing powder of these torches is less than believed. Under certain conditions, when air was used for powder feeding, deposits made from metal NiTi contained a significant amount of TiO_2. Similarly, NiAl oxides (Fig. 2c) and even nickel oxides were found by XRD in some deposits or in free-flight particles. On the other hand, spraying parameters exist where no oxides form when using air feeding, even when spraying aluminum powder.[9] When argon was used as a carrier gas, regardless of the material used, the amount of oxides diminished or was not detected at all. This result suggests that the oxidation is more likely to be connected to the type of feeding than to the oxidation power of the plasma itself.

4.3 *Processes on the Substrate*

4.3.1 *Formation of Microcrystalline and Amorphous Phases: $ZrSiO_4$*

A thin foil (Fig. 5) perpendicular to the steel substrate[10] was made from the first layer of $ZrSiO_4$ splats. Using TEM, SAD, and XRD, several structural types and phases were distinguished in the foil: (1) microcrystalline regions of ZrO_2 with two distinct grain sizes (25 to 50 nm and 50 to 100 nm) and an amorphous phase were found directly adjacent to the interface; (2) grains of ZrO_2 arranged into bands separated by a glassy SiO_2 phase; and (3) a crystalline residuum comprising the largest portion of the splat.

Splats farther away from the deposit/substrate interface contain less of the microcrystalline and amorphous phases, but also contain a transient structure of ZrO_2 resembling that of an annealed metallic glass. In the microcrystalline regions and layers next to the interface, only the high-temperature modifications (cubic and tetragonal) of ZrO_2 were detected as a consequence of the faster local cooling rates. The low-temperature monoclinic phase was found further away from the interface where the relative cooling rate was lower and grains of ZrO_2 were larger and thus more likely to transform.[11]

4.3.2 *Effect of Overall Cooling Rate: Al_2O_3*

The overall cooling rate can be the decisive factor regulating the final structural type and consequently the properties of a material in the plasma-sprayed deposit. For many applications, the only useful modification of Al_2O_3 is α phase, which is stable, hard, and resistant to many chemicals. However, under normal spraying circumstances, the metastable γ and δ phases usually form.[1,7,8] The most common method used to overcome this problem is chemical stabilization, but it is only successful to a certain degree. Heat treatment of the deposited coating is practically of no use. McPherson[1] proposes that, if αAl_2O_3 powder is only partially melted, the unmelted core of a particle can act as a nucleus for the formation of α phase after the impact. The free-flight particles with a longer spray distance contained more αAl_2O_3 than the deposit, supporting McPherson's proposal. On the other hand, γ phase is appropriate for some applications. It can be formed chemically,[12] or by a controlled cooling rate of the deposited coating. As a general rule for Al_2O_3 deposits, the higher the cooling rate, the higher the content of the γ fraction. In particles that are cooled at a lower cooling rate, the γ phase transforms to the more stable δ phase.

4.3.3 *Interface Diffusion*

A model experiment was carried out to discover the existence of the formation of special transition phases at the interface. A droplet of molten molybdenum fell by gravity onto a slightly preheated (100 °C) steel substrate. Figure 6 shows that a distinct phase formed with ~30 wt% Mo and ~70 wt% Fe. Conversely, careful examination of the Al_2O_3/steel substrate inter-

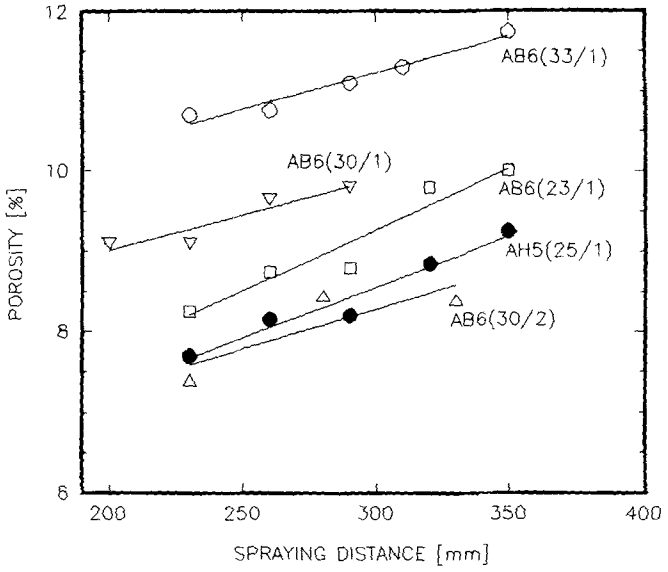

Figure 7 Porosity dependence with respect to the spraying distance. Letters denote various types of original Al_2O_3, numbers beside the letters denote the feeding distance divided by the number of injectors (*i.e.*, for material AH5, there was 1 injector at a feeding distance of 25 mm).

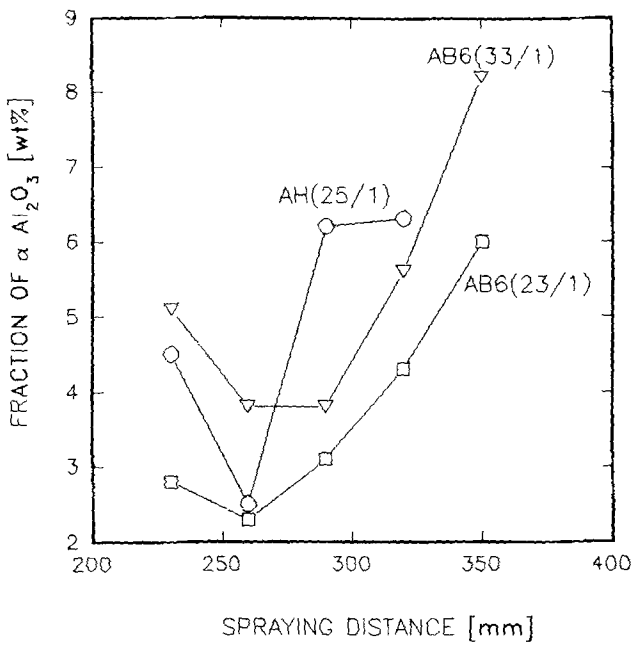

Figure 8 αAl_2O_3 content dependency with respect to the spraying distance. Letters and numbers denote the same as in Fig. 7.

face by XMA did not show any large-scale diffusion or formation of a transition phase.[13]

4.4 *Effect of Geometrical Setup*

Besides the spraying distance (see Fig. 1), which is an important parameter in any type of thermal spraying, the feeding distance (FD) is another important parameter pertinent to spraying systems with external feeding. Porosity of coatings (Fig. 7), as well as the maximum temperature of the substrate, is given by a combination of spraying distance and feeding distance.[9,14] The αAl_2O_3 content (Fig. 8) depends on spraying distance and feeding distance as well:[14] the longer the feeding distance, the higher the α fraction for any spraying distance used as indicated by a plot of the dependency of α phase with respect to spraying distance, which exhibits a distinct minimum. At the same time, a longer spraying distance results in a longer time of flight, which may be connected to the processes mentioned in Section 4.3.2.

5. Concluding Remarks

Many different phase changes occur during plasma spraying. Some of these may, to varying degrees, be pinpointed at a certain stage of the process. However, experimental review of many phases after spraying suggests that a large-scale redistribution of chemical elements occurs in the process. Because, generally, all the new phases are usually distributed at random, it is impossible in many cases to decide conclusively at what stage of this nonequilibrium process the main chemical redistribution takes place.

Phase changes in coatings on the substrate depend on the cooling rate of the flattening droplets and on the substrate temperature. Experimental determination of the latter may be performed with samples that have thermocouples mounted in holes near the sample surface. These were sprayed with various materials alongside regular samples, for different spraying distances, feeding distances, geometry, etc., and the temperature was recorded continuously. The temperature never exceeded 400 °C, but in most cases, the maximum was only around 200 °C. These results clearly suggest that no large-scale chemical redistribution is likely to take place on the substrate after solidification. Thus, the type of microstructure and the phase content obviously depend strongly on the cooling rate, which can vary from 10^2 to 10^6 K · s^{-1}.[11] For some materials (*e.g.*, Al_2O_3), the final structure is determined by the overall cooling rate, whereas other materials (*e.g.*, $ZrSiO_4$) are very sensitive to local rates of cooling. Consequently, microregions of different phases and structures can form even in a single splat, including the amorphous phase. Cooling rates in turn depend on the heat transfer at the interfaces between the splat substrate and/or between splats. These conditions are usually quite complex, varying from splat-to-splat and depending on many spraying parameters and variables.[15]

However, some phase changes definitely take place during the flight stage, which rarely exceeds 1 ms. As illustrated by the aluminum-silicon case (Section 4.2.1), this time is long enough for redistribution of aluminum and silicon. Formation of the aluminum-silicon eutectic even in the free-flight particles clearly indicates its "cooling-in" from the liquid state.

In conclusion, the phase composition and the type of microstructure can vary significantly for the same chemical composition of feedstock, depending on processing variables. This conclusion contests the oversimplifying approaches that attempt to regulate the final properties of a plasma-sprayed coating only by changing chemical composition of the feedstock powder. At the same time, it is equally clear that more work is

necessary in a number of fields such as particle/plasma interaction, chemical activity of water-stabilized plasma jets, modeling of heat transfer on impact, nonequilibrium phase changes, and stability of nonstoichiometric phases.

Acknowledgment

The authors express their thanks to K. Neufuss for spraying, P. Raus for TEM, J. Kaspar (Research Inst. of Met., Brno) for the molybdenum sample, and to other colleagues from IPP for their valuable help. Also, the comments of C. Berndt during the preparation of this article are gratefully acknowledged.

References

1. R. McPherson, On the Formation of Thermally Sprayed Alumina Coatings, *J. Mater. Sci.*, Vol 15, 1980, p 3141-3149.
2. P. Chraska, J. Dubsky, and K. Neufuss, Plasma Sprayed Alumina Coatings, *Proc. 2nd Metallography Conf.*, CSVTS, Karlovy Vary, 1985, p 509-514.
3. J. Zeman and M. Cepera, Phase and Structure Analysis of Ceramic Based on $ZrO_2 + Y_2O_3$, *Int. Rep. Res. Inst. Met. Brno*, No. 78-1/646, 1990.
4. P. Fauchais, J.F. Courdet, A. Vardelle, M. Vardelle, and J. Lesinski, Diagnostics under Thermal Plasma Conditions, in *Plasma Processing and Synthesis of Materials*, J. Szekely and D. Apelian, Ed., MRS Symposia, Vol 30, 1984, p 37-51.
5. D.A. Apelian, R.W. Smith, and D. Wei, Particle Melting and Droplet Consolidation During Low Pressure Plasma Deposition, *Powder Metall. Int.*, Vol 20, 1988, p 7-10.
6. J. Dubsky, P. Chraska, B. Kolman, and K. Neufuss, Protective Coatings from Al-Si on Graphite Electrodes, *Proc. 3rd Metallography Conf.*, CSVTS, Karlovy Vary, 1989, p 471-474.
7. J. Dubsky, B. Kolman, and P. Chraska, Effect of Cooling on the Phase Formations of Al_2O_3, *Proc. 7th Metallography Symp.*, CSVTS, High Tatras, 1989, p 168-171.
8. B. Kolman, P. Chraska, J. Dubsky, and M. Beranek, Comparison of Several Types of Al_2O_3 Based Powders for Spraying, *Proc. 4th Metallography Conf.*, CVSTS, Mar. Lazne, 1989, p 324-326.
9. J. Ilavsky, J. Forman, and P. Chraska, Plasma Sprayed Aluminium Coating, *Mater. Sci. Lett.*, Vol 11, 1992, p 573-574.
10. P. Raus and P. Chraska, Transmission Electron Microscope Study of a Plasma-Sprayed Zircon Coating, *Silikaty-Ceramics*, Vol 33, 1989, p 325-332.
11. F. Kroupa, Transformation Toughening of Ceramic, *Czech. J. Phys. A*, Vol 37, 1987, p 552-573.
12. N. Iwamoto, Y. Makino, and K. Tanaka, Fundamental Considerations on Plasma Sprayed Ceramic Coating (Report 2)—Structural Study of Plasma Sprayed Al_2O_3, *Trans. JWRI*, Vol 6, 1977, p 107-111.
13. J. Forman, J. Ilavsky, and P. Chraska, Comparison of Various Alumina Based Deposits Made by the Plasma Spraying Technique, *Proc. 5th Conf. Aluminium Oxide*, Czechoslovakia Scientific and Technical Society and Center of Materials Science, Prague Institute of Chemical Technology, Prague, 1990, p 59-64.
14. J. Ilavsky, K. Neufuss, and P. Chraska, Influence of Spraying Parameters on Properties of Al_2O_3, *Proc. 5th Conf. Aluminium Oxide*, Centre of Materials Science, Prague Inst. of Chem. Tech., 1990, p 65-70.
15. D. Apelian, M. Paliwal, R.W. Smith, and W.F. Schilling, Melting and Solidification in Plasma Spray Deposition—Phenomenological Review, *Int. Met. Rev.*, Vol 28, 1983, p 271-294.